Effect of Catalyst Deactivation on Polymerization of Electrolytes by Surface-Confined Atom Transfer Radical Polymerization in Aqueous Solutions

Amit Y. Sankhe, Scott M. Husson, and S. Michael Kilbey, II*

Department of Chemical and Biomolecular Engineering and Center for Advanced Engineering Fibers and Films, Clemson University, Clemson, South Carolina 29634-0909

Received September 5, 2005; Revised Manuscript Received October 21, 2005

ABSTRACT: We have investigated the cause of catalyst deactivation observed during surface-confined atom-transfer radical polymerization of acidic monomers. Surface-tethered polyelectrolyte layers of poly(itaconic acid) and poly(methacrylic acid) were grown from self-assembled initiator monolayers of 2-bromoisobutyryl bromide terminated thiol molecules. This polymerization initiator molecule and a copper-based organometallic catalyst allowed tethered polyelectrolyte chains to be grown directly via radical polymerization at room temperature in aqueous solutions. Structural and surface properties of the layers were characterized using phase-modulated ellipsometry and external-reflection Fourier transform infrared spectroscopy. Catalyst deactivation due to generation of a coordination complex between the deprotonated acid monomers and copper catalyst during the polymerization process appears to be an important cause of chain growth cessation. Surface-initiated polymerizations performed after aging of the catalyst-containing deprotonated monomer solution revealed inhibition of polymer growth with increasing aging times. This suggests that catalyst is consumed over time by complexation with carboxylate groups of the monomer and dissociation and disproportionation in water.

Introduction

Overcoming the deactivation of atom-transfer radical polymerization (ATRP) catalysts when polymerizing electrolytic or charged monomers continues to be a chemical challenge. Surmounting this challenge is important because surface-tethered layers of charged polymer have numerous applications including colloidal stabilization,[1] membrane preparations,[2] and biosensor and biomaterial scaffold technologies.[3,4] As a result, studying the structure and properties of carefully designed surface-tethered, charged polymer layers, also referred to as polyelectrolyte layers (PELs), has generated considerable theoretical and experimental interest.

The study of surface-tethered PELs would benefit from the development of procedures that simplify the formation of these charged interfacial layers on solid surfaces. A variety of approaches that build off methods used to prepare polymer brushes have been used to produce surface-tethered PELs. In general, polymer brushes can be formed on surfaces by using techniques such as physisorption of block copolymers,[5−8] covalent grafting of end-functionalized polymers,[9−11] and graft polymerization from the surface.[12] Each method has its utility: The "grafting from" approach produces end-tethered polymer brushes of higher thickness and grafting density compared to the "grafting to" approaches;[13] the latter faces the inherent weaknesses of slow diffusion of polymers to the surface and the entropy penalty associated with chain stretching to accommodate more chains.[14] Nevertheless, the "grafting to" approach is often preferred for fundamental studies because the molecular features and composition of the premade polymer chains can be rigorously characterized prior to grafting. Balastre et al. demonstrated[8] that the "grafting to" approach could be used to form PELs of polystyrene sulfonate by preferential assembly of poly(*tert*-butylstyrene)−poly(styrenesulfonate) diblock copolymers made by anionic polymerization onto a hydrophobicized surface.

* Corresponding author. E-mail: mkilbey@clemson.edu.

A two-step "grafting from" approach has been used by Rühe and co-workers to produce polyelectrolyte brushes of poly(1-methyl-4-vinylpyridinium iodide)[15] and poly(styrenesulfonate)[16] from surface-tethered azo initiators. In each case, a precursor neutral brush was synthesized by thermally initiated, free-radical polymerization and then subsequently converted to yield the polyelectrolyte brush. The poly(1-methyl-4-vinylpyridinium iodide) brush was prepared by first growing a brush of poly(4-vinylpyridine), and then the 4-vinylpyridine groups were quaternized with methyl iodide.[15] Poly(styrenesulfonate) brushes were formed by saponification of poly(*p*-styrenesulfonate ethyl ester) brushes.[16] Zhang and Rühe also demonstrated that polyelectrolyte brushes of poly(methacrylic acid) could be prepared directly by thermally initiated polymerization of methacrylic acid using surface-tethered azo initiators.[17] An alternative, two-step process to form PELs involving chemical modification of polyacrylate or polyester brushes was reported by Boyes et al.[18] In their work, uncharged polymer brushes bearing acrylate or ester pendent groups were grown in organic solvents by surface-confined ATRP (SC-ATRP) and then hydrolyzed in aqueous solution to form the corresponding acid brushes.

Although ATRP has been used widely for controlled polymerization of monomers with nonionic functionalities in aprotic solvents, and results such as those by Boyes et al.[18] and Biesalski et al.[15,16] demonstrate that polyelectrolyte brushes can be made by postpolymerization modification, it may be argued that methods to *directly* create tethered polyelectrolyte layers would be beneficial. Moreover, methods that allow ATRP of charged monomers to be carried out in an environmentally friendly solvent such as water in a controlled or "living" fashion would open the design envelope and allow well-defined interfacial polyelectrolyte layers to be made for a host of applications. However, there are known challenges associated with carrying out ATRP in water: Tsarevsky and Matyjaszewski point out in their studies of ATRP in bulk solution of cationic monomers and the neutral water-soluble monomer 2-hydroxyethyl meth-

10.1021/ma0519361 CCC: $33.50
Published on Web 01/26/2006

acrylate that catalyst deactivation by dissociation, complexation with monomers and solvent, and disproportionation occur readily in aqueous media.[19] These deleterious effects preclude achieving a "controlled" radical polymerization. Some of these problems can be circumvented by reducing the water content by adding an aprotic solvent or a ligand that stabilizes the copper halide complex. Iddon et al. demonstrated that ATRP of sodium 4-styrenesulfonate was uncontrolled in water, but control improved when the water content was decreased by adding methanol as a cosolvent; polydispersities as low as 1.26 and high conversions were obtained using a 1:1 mixture of water and methanol.[20]

This approach of adding an aprotic solvent was implemented by Moya et al. in their efforts to directly prepare polyelectrolyte brushes of [2-(methacryloyloxy)ethyl]trimethylammonium chloride via SC-ATRP in a methanol-rich aqueous solution.[21] In their work, quartz crystal microgravimetry (QCM) was used to follow the kinetics of layer growth. QCM results show a leveling off in change of frequency, meaning that the rate of mass addition to the tethered chains slows after an initial rapid growth period. This decrease in the rate of growth, as evidenced by the change in frequency, occurred quickly and is indicative of cessation of polymerization. Thus, even though a significant amount of aprotic solvent was added, ostensibly to overcome problems with catalyst deactivation, the characteristic linear increase in thickness of the layer with time that normally is cited as evidence of controlled growth via SC-ATRP was only seen in the case where a 4 nm thick layer (polymer and initiator) was grown using a low surface-initiator density.

To the best of our knowledge, the only report to date of a controlled ATRP of a charged monomer in water is that of Ashford et al.[22] They were able to use ATRP in a controlled fashion to polymerize methacrylic acid in water at 90 °C by using poly(ethylene oxide) macroinitators. Low molecular weight polymers (<7500 g/mol) were made with polydispersities of 1.2−1.3.

Thus, it may be concluded that devising situations to capitalize on the well-known robustness of ATRP for surface-confined polymerization of charged/ionic monomers in water remains particularly challenging. To take advantage of ATRP as a controlled/living polymerization technique capable of producing well-defined, end-functionalized or block copolymers, it is necessary to understand the side reactions that occur when attempting to polymerize charged monomers in water. These side reactions lead to the deactivation of catalyst by three routes: coordination complex formation between the catalyst and deprotonated monomer, disproportionation, and dissociation of the catalyst. In this article we report findings on the deactivation of catalyst that occurs during SC-ATRP of itaconic acid (IA) and methacrylic acid (MAA) in aqueous solutions.

Poly(itaconic acid) (PIA), a "green" material by virtue of being produced by bioorganisms,[23] has two carboxylic acid groups per monomer, which gives PIA a very high theoretical ion-exchange capacity. As a result, PIA may be used to create ion-exchange separation agents used as column packings to extract cations such as metal ions and organic dyes from solution.[24,25] Unlike PIA, poly(methacrylic acid) (PMAA) has one carboxylic acid group per repeat unit. Both monomers are weak electrolytes. Hence, the primary goals of the present study are to highlight the complexities involved in polymerizing electrolytic, anionic monomers such as IA and MAA using SC-ATRP and also to reveal the cause of depletion of active catalyst during ATRP of these acidic monomers. This information will ultimately aid in devising situations whereby controlled SC-ATRP can be carried out to directly produce well-defined polyelectrolyte brushes, thus furthering the study of these complex materials.

Experimental Section

Materials. Gold-coated silicon substrates were used for ATRP studies. A 1000 Å gold layer was sputter coated onto a 10 mm × 12 mm silicon wafer chip with a 100 Å binder layer of chromium between the silicon and gold. The following chemicals were purchased from Aldrich and used as received: tris(2-aminoethyl)-amine (TREN; 96%), sodium hydroxide (pellets, 98%), anhydrous ethanol (99.5%), copper(I) chloride (99.9%), 2-bromo-2-methyl-propionyl bromide (98%), methacrylic acid (MAA; 99%), and itaconic acid (IA; 99%). Methacrylic acid was purified by vacuum distillation before use. Itaconic acid was recrystallized from ethanol prior to use. The ligand hexamethyltris(2-aminoethyl)amine (Me_6-TREN) was synthesized by methylation of TREN.[26]

Bromo Initiator Synthesis and Self-Assembly. The bromo initiator ($BrC(CH_3)_2COO(CH_2)_{11}S)_2$, also referred as the polymerization initiation molecule (PIM), is self-assembled onto the gold surfaces and synthesized using the procedure developed by Shah et al.[27] Gold surfaces were cleaned using a Boekel ozonation chamber for 5 min before self-assembling the PIM. The monolayers were formed by placing the clean gold substrate in a 1 mmol solution of the bromo initiator in anhydrous ethanol under a continuous nitrogen purge for more than 16 h. The gold surfaces coated with self-assembled initiator monolayers were washed with ethanol, dried in a stream of nitrogen, and characterized using standard surface characterization techniques such as ellipsometry and external-reflection Fourier transform infrared (ER-FTIR) spectroscopy to confirm the presence of the surface-tethered initiator monolayer before polymerization. Results from self-assembled monolayer characterization studies were consistent with our previous studies[28] and therefore were not repeated here.

ATRP Chemistry. SC-ATRP was used for both acidic monomers, MAA and IA. The polymerization reaction used an organometallic catalyst complex comprising $Cu^{I}Cl$ and ligand Me_6TREN. A mixed halide system was used for the ATRP with the bromo initiator and $Cu^{I}Cl$ as the catalyst, because mixed halide systems are reported to have better control for ATRP.[29−31] The reaction medium was prepared inside a Schlenk flask. Acid monomers (IA = 2.6 g, 0.18 wt %; MAA = 1.72 g, 0.13 wt %) were first added to 10 mL of water. The acid monomers were then deprotonated by adding NaOH (1.6 g for IA and 1.2 g for MAA) to reach a pH endpoint of 7.0 (±0.1). Me_6TREN (0.23 mg) and $Cu^{I}Cl$ (49.5 μg) were then added to the deprotonated monomer solution to form the reaction medium. The reaction media was degassed inside the Schlenk flask by multiple freeze−pump−thaw cycles to ensure that dissolved oxygen (which can terminate polymerization) was removed completely from the reaction solution. Aliquots of the reaction medium were then transferred to different test tubes inside an oxygen-free glovebox, and the PIM-modified gold surfaces were placed inside the test tubes. The polymerization proceeded at room temperature for various polymerization times up to 60 h. Following polymerization, the surfaces were removed from the monomer/catalyst solution, washed with water, and dried with a stream of nitrogen prior to characterization experiments. The effect of aging was studied by letting the reaction medium containing the deprotonated monomer and catalyst age inside the glovebox for different predetermined times. Aliquots of the aged reaction media were then transferred into test tubes that contained the PIM-modified gold surfaces, and the polymerization was carried out inside the glovebox for various polymerization times.

Surface Characterization Techniques. Standard surface characterization techniques were used to study the structure and the surface properties of the modified surfaces. The ER-FTIR analysis was performed using a Nicolet Nexus 870 with a Spectra-Tech FT-80 Horizontal Grazing Angle accessory with an 80° fixed incidence angle. The spectra were collected at room temperature with a liquid nitrogen cooled MCT-A detector. For each sample, at least 2000

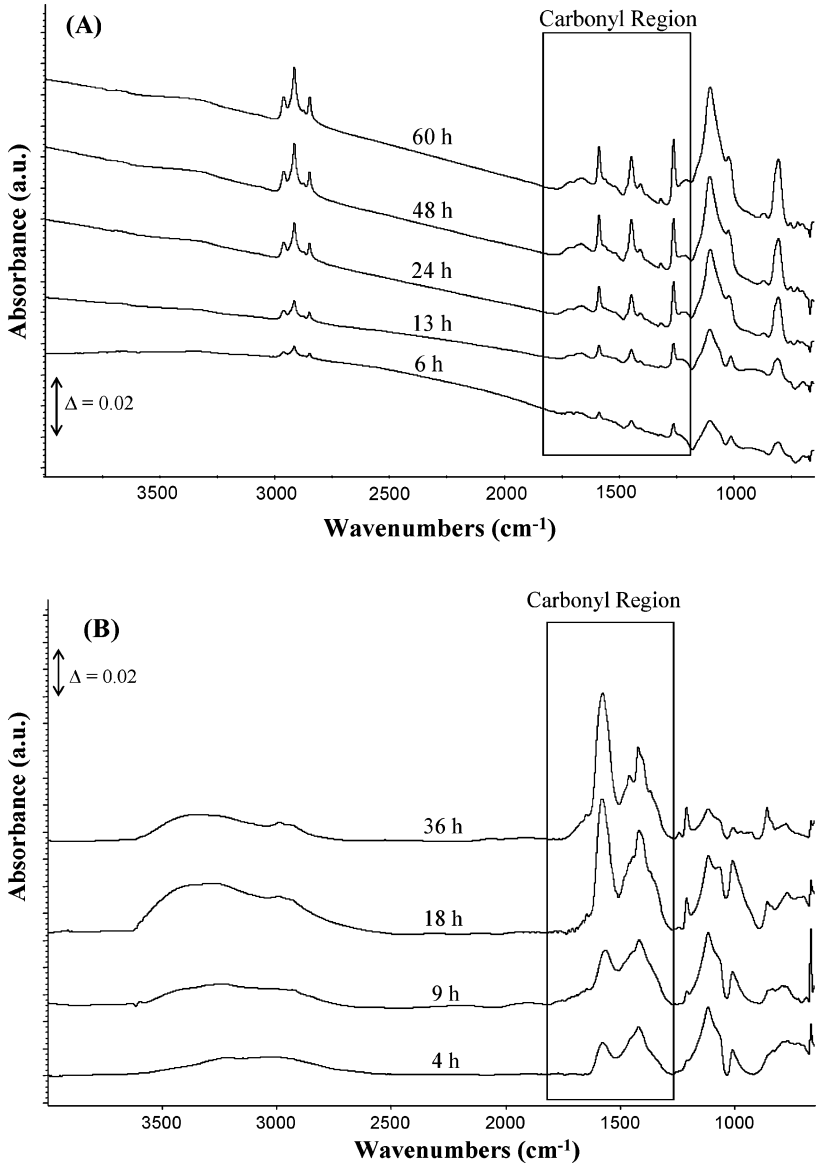

Figure 1. External-reflection FTIR spectra of poly(itaconic acid) layers (A) and poly(methacrylic acid) (B) on gold surfaces gathered at different polymerization times. Polymer-coated surfaces prepared by surface-initiated atom-transfer radical polymerization in aqueous solutions with 1:2 molar equivalents of $Cu^{I}Cl/Me_6TREN$ and either 0.18 wt % itaconic acid or 0.13 wt % methacrylic acid at room temperature.

scans were collected, with a resolution of 8 cm^{-1}. A Whatman laboratory gas generator (Model 75-45) was used to purge the sample compartment with dry, CO_2-free air.

Layer thickness was measured using a Beaglehole Instruments Picometer Ellipsometer, which uses a photoelastic crystal modulator and a He−Ne laser (λ = 632.8 nm). Measurements were done at five separate spots on each sample (with standard deviations represented by the error bars in Figures 2 and 3) with an assumed refractive index of 1.45 for the bromo initiator, 1.5 for PIA, and 1.4 for PMAA. Data were collected by varying the angle of incidence of the laser from 80° to 35° using steps of 1.0° (angular resolution of ±0.1°).

Results and Discussion

SC-ATRP of Acidic Monomers. The progress of each polymerization reaction was followed by measuring the dry layer thickness with phase-modulated ellipsometry and the corresponding changes in absorbance using ER-FTIR spectrometry. Monomers containing deprotonated carboxylic acid functionalities were polymerized directly from gold surfaces in an aqueous medium. Although growth of the polymer layer on the surface was observed, it stopped abruptly after a brief propagation period. According to Figure 1A, the ER-FTIR spectra obtained for the polymerization of IA at different polymerization times show a steady increase in peak intensities until around 24 h but not more than 48 h, and remain unchanged thereafter. Peaks obtained at 1586 and 1407 cm^{-1} represent the carboxylate anion stretching observed from the deprotonated acid groups of the PIA.[32] Also, peaks due to C−O stretching are present at 1446 and 1262 cm^{-1}.[32] The stacked spectra confirm the presence of PIA on the gold surface and that the growth of PIA halts after a brief propagation period. Similar studies were done with MAA to test the generality of these findings for deprotonated acidic monomers. ER-FTIR spectra show increasing intensities of carboxylate anion stretching peaks at 1580 and 1420 cm^{-1} for polymerization times until ~9 h but not more than 18 h, and remain unchanged thereafter (Figure 1B).

To complement the ER-FTIR results, polymer dry layer thicknesses were measured at different polymerization times using phase-modulated ellipsometry. As shown in Figure 2, there is a rapid initial growth of the PIA layer, but growth stops after ~24 h of polymerization, as manifested by the plateau. The thicknesses measured include the thickness of the initiator

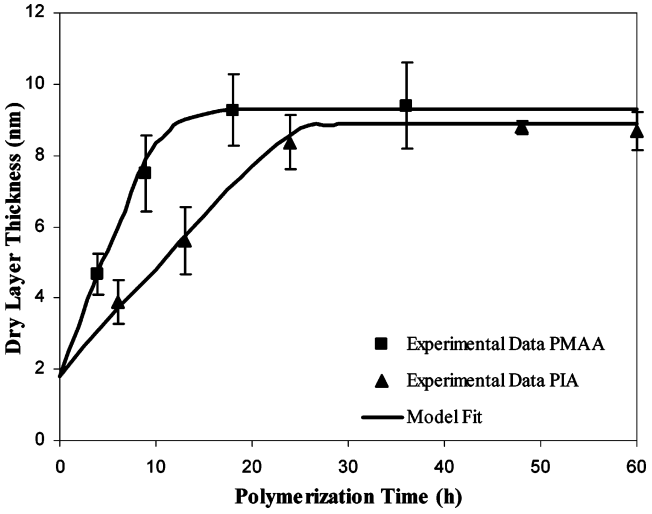

Figure 2. Ellipsometric dry layer thickness measurements showing growth kinetics of poly(methacrylic acid) and poly(itaconic acid) layers. Polymer-coated surfaces prepared by surface-initiated atom-transfer radical polymerization in aqueous solutions with 1:2 molar equivalents of $Cu^{I}Cl/Me_6TREN$ and either 0.18 wt % itaconic acid or 0.13 wt % methacrylic acid at room temperature. The lines represent fits using the model expressed by eq 4.

Scheme 1. Scheme Illustrating a Possible Atom-Transfer Radical Polymerization Catalyst Deactivation Process by Complexation with the Deprotonated Acid Monomer

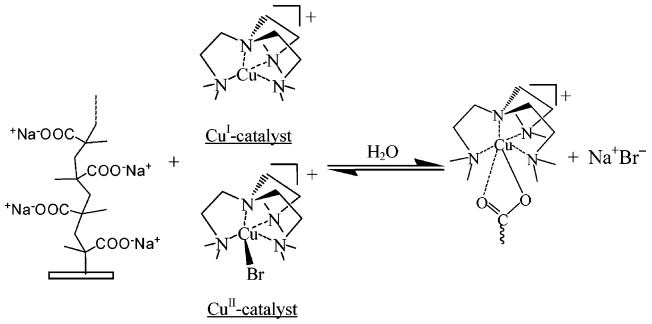

monolayer, which was measured to be 1.8 nm.[28] PIA layers achieve thicknesses of 8 nm before complete cessation of growth. The ellipsometric thickness measurements for PMAA layers show growth to a dry layer thickness of ~9 nm and the time for attainment of the plateau is between 10 and 16 h (Figure 2). PMAA grows faster than PIA because PMAA has a higher rate of propagation (1.7 L mol^{-1} s^{-1} for PIA and 670 L mol^{-1} s^{-1} for PMAA, obtained from studies of conventional solution radical polymerization).[33]

After examining both ER-FTIR and ellipsometry results, and also as will be demonstrated later with the aging studies, we hypothesize that, in addition to undergoing dissociation and disproportionation in water, SC-ATRP copper catalyst can form coordination complexes with MAA and IA (Scheme 1), causing depletion of the catalyst and thus deterring the polymerization. Gradual depletion of the catalyst occurs and, when it is consumed completely, a plateau is reached and cessation of polymerization occurs.

The behavior of ATRP catalyst in a reaction system containing polar monomers and protic solvents is complex. Basically, ATRP depends on the reversible reaction of the alkyl halide RX (X = Br, Cl) and the cuprous complex $Cu^{I}Y/L$ (Y = Cl, Br; L = ligand) to produce radicals and a higher oxidation state cupric complex ($XCu^{II}Y/L$) with the extracted halide.[31] The reversible switching between the lower oxidation state complex ($Cu^{I}Y/L$) and the higher oxidation complex ($XCu^{II}Y/L$) is

Scheme 2. Reaction Scheme Illustrating the Effects of Water on Catalyst Depletion

$$2\ Cu^{I}Y/L \rightleftharpoons Cu^{II}Y_2/L + Cu + L$$

$$XCu^{II}Y/L + (m+1)H_2O \rightleftharpoons X(H_2O)_m + (H_2O)\text{----}Cu^{II}Y/L$$

essential for controlled ATRP. Hence, the presence of the deactivator, $XCu^{II}Y/L$, is necessary to establish and maintain the reaction equilibrium. Any deviations from this equilibrium may cause the termination of polymerization or may result in uncontrolled polymerization kinetics. In the case of SC-ATRP, the $XCu^{II}Y/L$ provides control by maintaining a low radical concentration on the surface.[31] Radicals that form can react by adding to the double bond of a monomer, irreversible termination by bimolecular coupling or disproportionation, or reversible deactivation by halogen exchange from the $XCu^{II}Y/L$ complex. Since the equilibrium favors the dormant species, the presence of $XCu^{II}Y/L$ suppresses radical−radical coupling, giving ATRP its "controllable" nature. Unfortunately, in aqueous systems with charged monomers, two mechanisms exist for depletion of $XCu^{II}Y/L$. These include ion exchange and dissociation, as discussed below.

Both IA and MAA are acidic monomers. Deprotonation of these monomers with NaOH forms ionic functionalities that can poison the ATRP catalyst by ion exchange.[34,35] A carboxylate group displaces a halide ion from $XCu^{II}Y/L$ to form a $-Cu^{II}Y/L-$carboxylate complex. The high affinity of carboxylate ions to copper ions over sodium ions is responsible for this ion exchange.[36] The complexation of the growing acid polymer with the $XCu^{II}Y/L$ complex results in release of sodium ions from the deprotonated acid monomer and displacement of the halogen atom from the catalyst complex. The displaced halogen forms an ion pair with sodium ion in the aqueous reaction medium as indicated in Scheme 1.

Although the use of water as solvent makes ATRP more environmentally friendly, the deactivation of ATRP catalysts by hydrolytic solvation makes aqueous systems difficult to use.[19] The higher oxidation state copper complex $XCu^{II}Y/L$ dissociates easily in water. Water forms a coordination complex with $Cu^{II}Y/L$ by displacing a halide atom, thereby reducing the concentration of the deactivator (Scheme 2). This process also exhausts the deactivator, which indirectly leads to the depletion of Cu^{I} according to the reaction equilibrium. Also, the lower oxidation state copper complex $Cu^{I}Y/L$ can disproportionate in the presence of water and ionic monomers.[19] Disproportionation of $Cu^{I}Y/L$ halts radical formation, which stops the polymerization. Loss of the deactivator causes chain growth cessation by allowing bimolecular coupling to take place more readily.

Bimolecular termination involves the coupling of chain-end radicals from two neighboring chains. This termination event occurs more readily when the chains are in short supply of the halogen atoms needed to reversibly cap them. The reversible equilibrium between the Cu^{I} and Cu^{II} complexes ensures that, after short sequences of repeat unit (monomer) additions to the growing polymer chain, the chain end is capped with the halogen atom. Therefore, when the halogen atoms are consumed irreversibly by displacement from $XCu^{II}Y/L$, the growing chains can no longer be capped by the halogen atoms. The subsequent accumulation of polymer chain radicals promotes bimolecular termination (which is second order in radical concentration) and stops polymerization. For these reasons, both bimolecular termination and catalyst deactivation must be accounted for in any model to describe the growth rate behavior.

Modeling Layer Growth Kinetics. A kinetic model was developed to describe polymer growth. Details of the model

derivation are given in the Appendix. Briefly, the increase in film thickness, T, with time, t, is proportional to the monomer concentration, $C_{monomer}$, catalyst concentration, C_{cat}, and active chain concentration, C_{chains}.

$$\frac{dT}{dt} = k_p' C_{monomer} C_{cat} C_{chains} \quad (1)$$

In eq 1, k_p' represents the apparent propagation constant, and monomer concentration is a constant for controlled polymerization of ultrathin films from flat, low surface area substrates.[37,38]

If polymerization were "living" in the perfect sense, then active chain concentration would also remain constant. However, active chain concentration decreases due to bimolecular radical coupling and chain transfer side reactions.[39] To account for loss of active chains, we introduce a kinetic expression (eq 2) that describes bimolecular radical coupling of two active chains leading to polymer growth cessation; k_2 is the chain termination constant.

$$\frac{dC_{chains}}{dt} = -k_2 C_{chains}^2 \quad (2)$$

As discussed, catalyst deactivation can occur in aqueous ATRP by complexation with the monomer and by disproportionation in water. The loss of catalyst is assumed to be first order with respect to catalyst concentration (Schemes 1 and 2). Because the concentrations of monomer and water are in large excess relative to the catalyst concentration, they are assumed to be constant. As shown in the Appendix, the rate of catalyst deactivation can be written as shown in eq 3, with k_3 being an effective deactivation rate constant.

$$\frac{dC_{cat}}{dt} = -k_3 C_{cat} \quad (3)$$

Integration of eqs 2 and 3 leads to time-dependent expressions for the concentrations of the active polymer chains and catalyst. These expressions can be substituted into eq 1 and the resultant expression integrated to give a relationship between layer thickness and time (eq 4).

$$T = T_{PIM} + C\left[\log\left((1 + Bt) - DBt + \frac{D^2}{4}((1 + Bt)^2 - 1)\right)\right] \quad (4)$$

In eq 4, T_{PIM} is the thickness of PIM monolayer (measured previously[28] to be 1.8 nm) and the parameters A, B, C, and D collect the kinetic constants.

$$A = k_p' C_{monomer} C_{cat}^o C_{chains}^o$$

$$B = k_2 C_{chains}^o$$

$$C = \frac{A}{B} e^D$$

$$D = \frac{k_3}{B}$$

In these expressions the superscript "o" represents the initial value of the previously defined variables. Equation 4 is a truncated form of the exact solution, which allows data fitting to the short polymerization times used in this work. Extension of this model to longer polymerization times is cautioned.

The solid curves in Figure 2 represent the best fits of the model to the experimental data, showing that the model is rational and well-suited to describe the growth rate behavior for the polymerization times used in this study. The model described above was designed for surface-confined radical polymerization from a *low surface area* substrate and is not an accurate representation for solution polymerization or for surface polymerization involving high surface areas, because it assumes constant monomer concentration. For a self-assembled monolayer of the initiator on a gold surface of area 1 cm^2, the molar amount of initiator on the surface would be $\sim 7 \times 10^{-10}$ mol based on known self-assembled monolayer chain densities.[37,40] This low initiator density and low polymer layer thicknesses suggest that monomer consumption is negligible during polymerization.

The model fit yields k_p' values (3.3×10^4 M^{-2} h^{-1} for PMAA and 1.5×10^3 M^{-2} h^{-1} for PIA) that are orders of magnitude lower than the reported values for k_p' obtained from solution polymerization studies of neutral monomers (10^8 M^{-2} h^{-1}).[41,42] These apparent k_p' values for MAA and IA agree with the observation that the rate of polymerization of MAA is greater than that of IA. Differences between the apparent propagation rate constants and values for neutral monomers can be attributed to differences in polymerization conditions such as temperature, solvent, and monomer. Perhaps more importantly, the literature values are for solution polymerization. In the case of surface-initiated polymerization, access of monomer and catalyst to the surface may be diffusion limited, chain ends may become buried in the polymer layer, and deactivator may be present at higher concentrations near the surface where it forms.[39] These factors would all lead to lower apparent propagation rates for surface-confined polymerization compared to solution polymerization.

The growth curves in Figure 2 do not distinguish between the two mechanisms for polymerization termination. These curves represent the combined effect of catalyst deactivation and bimolecular termination on growth rate kinetics of surface-tethered polymers. Hence, to verify the effect of catalyst deactivation separately, we designed and performed experiments in which the reaction media were aged prior to use. Aging the catalyst-containing reaction media allows time for the catalyst to deactivate by interactions with the deprotonated monomer and water, but bimolecular chain coupling does not occur in the reaction medium due to the absence of the initiator radicals in the medium.

Aging Studies To Verify Catalyst Deactivation. As seen in Figure 2, during SC-ATRP, IA reaches a plateau by ~24 h and MAA by ~14 h (nominally). To verify the importance of catalyst deactivation in these uncontrolled polymerizations, aging studies were performed for both IA and MAA monomers. Reaction media containing the deprotonated monomer and Cu^I catalyst coordination complex were aged in a nitrogen glovebox for different lengths of time prior to polymerization. By aging the reaction medium, we are effectively allowing time for the catalyst to deactivate. The extent of deactivation depends on the aging time of the reaction medium: longer aging times imply greater complexation and disproportionation, and hence more extensive catalyst deactivation. The aged solutions were used in polymerizations to study the impact on layer growth kinetics.

The solutions containing IA were allowed to age for 6, 12, and 18 h (plateau by ~24 h), and the solutions containing MAA were aged for 3, 6, and 9 h (plateau by ~14 h). Using each aged solution, SC-ATRP of IA was carried out for 6, 12, 18, and 24 h. For MAA, SC-ATRP was carried out for 3, 6, 9, and

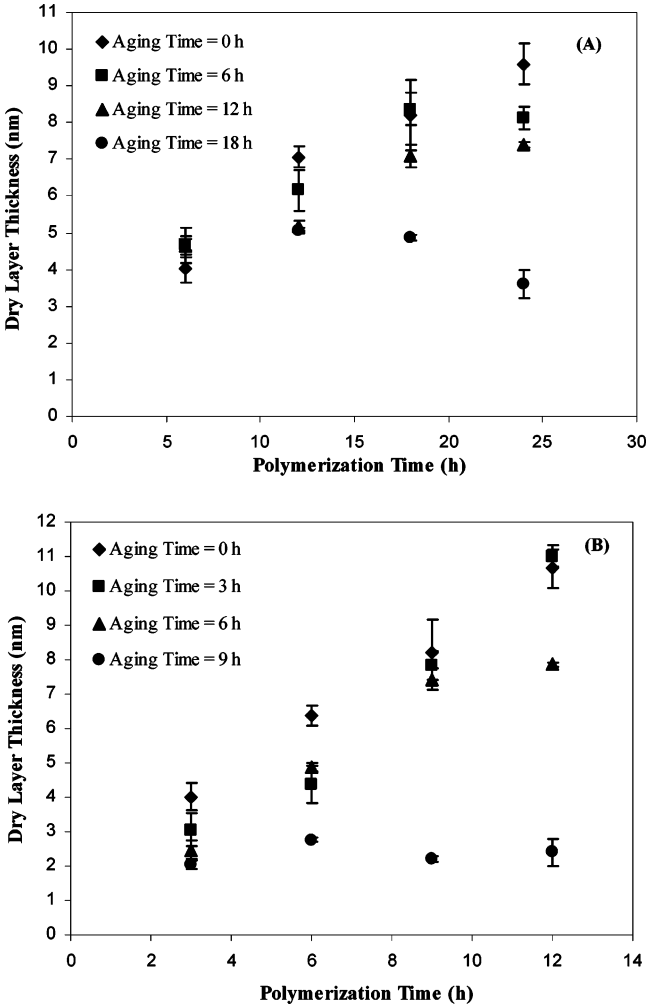

Figure 3. Dry layer thickness measurements showing growth kinetics of poly(itaconic acid) (A) and poly(methacrylic acid) (B) layers after aging monomer/catalyst solutions. Polymer-coated surfaces prepared from aged reaction media containing aqueous solutions of deprotonated acid monomers with 1:2 molar equivalents of $Cu^{I}Cl/Me_6TREN$ and either 0.18 wt % itaconic acid or 0.13 wt % methacrylic acid at room temperature. The reaction media were aged in an oxygen-free glovebox.

12 h. We hypothesized that, as aging time increases, the layer thickness achieved after surface-initiated polymerization will decrease and the plateau will be reached at earlier times.

Figure 3A shows dry layer thickness measured for surface-tethered PIA layers for different aging and polymerization times. When polymerization was done without pre-aging the reaction medium, the layer thickness increased linearly up to 24 h, which represents the transition time from the growth region to the plateau region for IA in Figure 2. In this case, the total time of catalyst exposure to monomer was less than this transition time. However, when the reaction medium is aged for 6 h prior to polymerization, layer thickness increases up to 18 h of polymerization, but does not further increase from 18 to 24 h. In this case, the maximum total time of catalyst exposure to monomer (30 h) exceeds the transition time (~24 h) from the growth region of Figure 2 to the plateau region. Similar trends were observed, with lower final layer thicknesses and quicker attainment of plateaus, with progressively increasing aging times. These results suggest that, as the reaction medium ages, catalyst deactivates by interaction with the charged monomer and disproportionation with water.

Figure 3B shows results obtained from similar aging experiments performed with MAA. From Figure 2, the transition from the initial growth region to the plateau region occurs between 12 and 18 h for PMAA. As seen in Figure 3B, increasing aging times result in lower layer thicknesses, and the crossover from the growth region to the plateau region also occurs faster.

When the reaction media age, side reactions occurring between the catalyst and the charged monomer and disproportionation of the $Cu^{I}Y/L$ complex lead to partial or complete depletion of the catalyst, depending on the length of aging time. When aged solutions subsequently are used for polymerization, reduced chain growth occurs due to deactivation of ATRP catalyst in the reaction solution. Figure 3 shows clearly that lower thicknesses and shorter times to reach a plateau result from solutions aged to longer times. The fact that some polymer grows suggests that not all of the $Cu^{I}Y/L$ disproportionates within the aging plus reaction times. Deactivation of the ATRP catalyst continues during the actual surface polymerization process, which leads to complete loss of active catalyst. Once the catalyst is deactivated, polymer ceases to grow. The time to reach deactivation is defined by the transition point from the growth region to the plateau region; this time correlates well with the overall time of catalyst exposure to monomer, which includes the aging time plus the polymerization time. The strong correlation between aging time and time to reach plateau thicknesses in both systems suggests that catalyst deactivation is a primary cause for cessation of layer growth. If the primary cause of cessation was bimolecular termination or chain transfer to solvent, then aging the solution would not markedly affect the growth behavior of surface-tethered chains.

Overall, both the carboxylate monomers (IA and MAA) and the aqueous medium contribute to the consumption of $Cu^{I}Y/L$ and the deactivator $XCu^{II}Y/L$ and, in turn, the exchangeable halide atoms. The ATRP system therefore is in short supply of the halide and the deactivator complex necessary for controlling the polymer growth. As the deactivator is consumed, halide exchange necessary for regeneration of the radicals does not occur, enhancing bimolecular termination. Although the mechanism by which catalyst deactivation occurs depends on solvent quality, the ligand used,[19] and the type of monomer, this study provides insight into possible ways to minimize deactivation by modifying the chemistry of the ATRP process. In the follow-on to this study we will describe a strategy to overcome this limitation of ATRP to polymerize charged electrolytic monomers in aqueous solutions.

Conclusions

Growth rate studies with the charged monomers IA and MAA, which suggest a catalyst deactivation mechanism by which cessation (of polymerization) occurs in ATRP systems, are presented. Infrared spectra reveal the occurrence of polymer growth termination by the saturation in the peak intensities at sufficiently long times. These results are well supported by ellipsometric data that show a plateau region of the measured dry layer thickness. Furthermore, pre-aging the reaction medium followed by polymerization provided additional experimental evidence about the role of catalyst deactivation in chain growth cessation. Polymer growth was inhibited with increasing aging times as exposure of the catalyst to deprotonated monomer solution during the aging process allowed time for catalyst deactivation side reactions to occur. These results establish that, during ATRP of carboxylate-functionalized monomers, several side reactions that occur between the monomer, solvent, and the copper catalyst complex lead to inefficient control and faster termination of polymerization.

Acknowledgments. We gratefully acknowledge the Engineering Research Centers Program of the National Science Foundation for financial support under NSF Award No. EEC-9731680. S.M.K. also thanks Nicholay Tsarevsky for helpful discussions.

Appendix. Kinetic Rate Model Derivation

Equation A1 describes the generalized ATRP rate equation. The rate of polymerization is first order with respect to monomer concentration, $C_{monomer}$, catalyst (Cu^I) concentration, C_{cat}, and the concentration of the active polymer chains, C_{chains}:

$$R_p = k_p'' C_{monomer} C_{cat} C_{chains} \quad \text{(A1)}$$

In eq A1, the apparent propagation rate constant, k_p'', represents the multiplication product of the true propagation constant, k_p, and K_{eq}^{app}, which has been defined by Matyjaszewski to be $K_{eq}^{app} = k_a/(k_d[Cu^{II}])$.[41] In this way, k_p'' in eq A1 has units of $M^{-2}\ h^{-1}$. The rate of polymerization can be expressed in terms of thickness, T, of the growing polymer brushes through a proportionality constant, β, that converts the rate of polymerization to the rate of thickness change and allowes the chain concentration to be given in units of moles/area, rather than molarity:

$$\frac{dT}{dt} = \beta\, k_p'' C_{monomer} C_{cat} C_{chains} \quad \text{(A2)}$$

Equation A2 can be recast as eq A3, where β and k_p'' have been grouped together as k_p'. This grouping was done in order to give a rate expression with equivalent form to eq A1 and with a rate constant that has the same units ($M^{-2}\ h^{-1}$) for meaningful comparison.

$$\frac{dT}{dt} = k_p' C_{monomer} C_{cat} C_{chains} \quad \text{(A3)}$$

The loss of active chains that occurs through radical−radical bimolecular coupling is second order with respect to active chain concentration, as described by eq A4.

$$\frac{dC_{chains}}{dt} = -k_2 C_{chains}^2 \quad \text{(A4)}$$

Integration of eq A4 gives eq A5 where C_{chains}° is the initial concentration of active chains on the surface.

$$C_{chains} = \frac{C_{chains}^\circ}{1 + k_2 C_{chains}^\circ t} \quad \text{(A5)}$$

We have shown in our SC-ATRP studies that side reactions that occur during ATRP in aqueous solution with anionic monomers, including disproportionation, deactivation (Scheme 2), and complexation with monomer (Scheme 1), may lead to loss of catalyst. The rate of change in catalyst concentration is assumed to be first order with respect to catalyst concentration and is represented by eq A6.

$$\frac{dC_{cat}}{dt} = -k_3' C_{monomer} C_{cat} - k_3'' C_{water} C_{cat} \quad \text{(A6)}$$

Because the monomer and water are in large excess relative to the catalyst, the concentration of the monomer and water are assumed to remain constant. This allows eq A6 to be recast as

$$\frac{dC_{cat}}{dt} = -(k_3' C_{monomer} + k_3'' C_{water}) C_{cat} \quad \text{(A7)}$$

Further simplification results by lumping the constants in parentheses into a single constant, k_3.

$$\frac{dC_{cat}}{dt} = -k_3 C_{cat} \quad \text{(A8)}$$

Integration of eq A8 gives eq A9, where C_{cat}° is the initial concentration of the catalyst in solution.

$$C_{cat} = C_{cat}^\circ\, e^{-k_3 t} \quad \text{(A9)}$$

Substituting eqs A5 and A9 in eq A3 yields eq A10.

$$\frac{dT}{dt} = k_p' C_{monomer} \left(\frac{C_{chains}^\circ}{1 + k_2 C_{chains}^\circ t} \right) C_{cat}^\circ\, e^{-k_3 t} \quad \text{(A10)}$$

Equation A10 can be recast in a simpler form, as shown as eq A11.

$$\frac{dT}{dt} = A\left(\frac{e^{-k_3 t}}{1 + Bt} \right) \quad \text{(A11)}$$

The constants A and B are defined as follows:

$$A = k_p' C_{monomer} C_{cat}^\circ C_{chains}^\circ$$

$$B = k_2 C_{chains}^\circ$$

Integrating eq A11 by parts and using the initial condition that $T = T_{PIM}$ at $t = 0$ yields a power series, which has been truncated to include only terms up to second order.

$$T = T_{PIM} + C\left[\log\left((1 + Bt) - DBt + \frac{D^2}{4}((1 + Bt)^2 - 1) \right) \right] \quad \text{(A12)}$$

The thickness of the surface-tethered initiator monolayer, T_{PIM}, is fixed at 1.8 nm (measured using ellipsometry[28]), and the constants C and D are defined as follows:

$$C = \frac{A}{B}\, e^D$$

$$D = \frac{k_3}{B}$$

A, B, and D in eq A12 were regressed to fit the ellipsometric experimental data of dry layer thicknesses of the surface-tethered polyelectrolyte. Evaluation of k_p' and other reaction parameters was done using A, B, C, and D and by using fixed values for initial catalyst, monomer, and chain concentrations. Fixed monomer concentration was used because surface-confined polymerization from low surface area substrates consumes a negligible amount of monomer relative to the starting amount in solution.[37] For initial chain concentration, we used the estimated areal density of initiator molecules on the surface (7×10^{-10} mol/cm^2) and assumed an initiator efficiency of 2% based on previous work by Samadi et al.[43] The curves in Figure 2 represent the kinetic model fits, with values of k_p' reported in the paper.

As a basis of comparison, Coullerez et al.[42] report data for k_p^{app} ($= k_p''[Cu^I][I]$) for copper complexes in oligoethylene glycol/water at room temperature. The reported value for the CuBr/Me_6TREN system was $k_p^{app} = 12.96\ h^{-1}$ using $[Cu^I] =$

$[I] = 2 \times 10^{-4}$ M. Using the relationship between k_p^{app} and k_p'', k_p'' was calculated to be 3.24×10^8 M^{-2} h^{-1}.

References and Notes

(1) Dautzenberg, H.; Jaeger, W.; Kötz, J.; Philipp, B.; Seidel, C.; Stscherbina, D. *Polyelectrolytes: Formation, Characterization and Applications*; Hanser: New York, 1994.
(2) Ding, J.; Chuy, C.; Holdcroft, S. *Chem. Mater.* **2001**, *13*, 2231−2233.
(3) Nakamura, H.; Karube, I. *Anal. Bioanal. Chem.* **2003**, *377*, 446−468.
(4) Zhu, H.; Ji, J.; Shen, J. *Biomacromolecules* **2004**, *5*, 1933−1939.
(5) Halperin, A.; Tirrell, M.; Lodge, T. P. *Adv. Polym. Sci.* **1992**, *100*, 31−71.
(6) Kilbey, S. M., II; Watanabe, H.; Tirrell, M. *Macromolecules* **2001**, *34*, 5249−5259.
(7) Dhinojwala, A.; Granick, S. *Macromolecules* **1997**, *30*, 1079−1085.
(8) Balastre, M.; Li, F.; Schorr, P.; Yang, J.; Mays, J.; Tirrell, M. *Macromolecules* **2002**, *35*, 9480−9486.
(9) Klein, M. J.; Kamiyama, Y.; Yoshizawa, H.; Israelachvili, J.; Fredrickson, G.; Pincus, P.; Fetters, L. *Macromolecules* **2000**, *33*, 5608−5612.
(10) Auroy, P.; Mir, Y.; Auvray, L. *Phys. Rev. Lett.* **1992**, *69*, 93−95.
(11) Karim, A.; Satija, S. K.; Douglas, J. F.; Ankner, J. F.; Fetter, L. J. *Phys. Rev. Lett.* **1994**, *73*, 3407−3410.
(12) Zhao, B.; Brittain, W. J. *Prog. Polym. Sci.* **2000**, *25*, 677−710.
(13) Biesalski, M.; Johannsmann, D.; Rühe, J. *J. Chem. Phys.* **2002**, *117*, 4988−4994.
(14) Toomey, R.; Mays, J.; Tirrell, M. *Macromolecules* **2004**, *37*, 905−911.
(15) Biesalski, M.; Johannsmann, D.; Rühe, J. *J. Chem. Phys.* **2004**, *120*, 8807−8814.
(16) Biesalski, M.; Rühe, J. *Macromolecules* **2003**, *36*, 1222−1227.
(17) Zhang, H.; Rühe, J. *Macromol. Rapid Commun.* **2003**, *24*, 576−579.
(18) Boyes, S. G.; Akgun, B.; Brittain, W. J.; Foster, M. D. *Macromolecules* **2003**, *36*, 9539−9548.
(19) Tsarevsky, N. V.; Pintauer, T.; Matyjaszewski, K. *Macromolecules* **2004**, *37*, 9768−9778.
(20) Iddon, P.; Robinson, K.; Armes, S. *Polymer* **2004**, *45*, 759−768.
(21) Moya, S. E.; Brown, A. A.; Azzaroni, O.; Huck, W. T. S. *Macromol. Rapid Commun.* **2005**, *26*, 1117−1121.
(22) Ashford, E. J.; Naldi, V.; O'Dell, R.; Billingham, N. C.; Armes, S. P. *Chem. Commun.* **1999**, *14*, 1285−1286.
(23) Bonnarme, P.; Gillet, B.; Sepulchre, A.; Beloeil, J.; Ducrocq, C. *J. Bacteriol.* **1995**, *177*, 3573−3578.
(24) Nagai, S.; Ueda, A.; Toyoda, K. U.S. Patent 4,245,053, Jan 13, 1981.
(25) Hull, E.; Leach, J.; Tate, B. U.S. Patent 3,219,596, Nov 23, 1965.
(26) Ciampolini, M.; Nardi, N. *Inorg. Chem.* **1966**, *5*, 41−44.
(27) Shah, R.; Merreceyes, D.; Husemann, M.; Rees, I.; Abbott, N.; Hawker, C.; Hedrick, J. *Macromolecules* **2000**, *33*, 597−605.
(28) Sankhe, A. Y.; Booth, B. D.; Wiker, N. J.; Kilbey, S. M., II. *Langmuir* **2005**, *21*, 5332−5336.
(29) Matyjaszewski, K. *Controlled/Living Radical Polymerization: Progress in ATRP, NMP, and RAFT*; American Chemical Society: Washington, DC, 2000.
(30) Qiu, J.; Charleux, B.; Matyjaszewski, K. *Prog. Polym. Sci.* **2001**, *26*, 2083−2134.
(31) Matyjaszewski, K.; Xia, J. *Chem. Rev.* **2001**, *101*, 2921−2990.
(32) Bellamy, L. *The Infrared Spectra of Complex Molecules*, 2nd ed.; Wiley: New York, 1958.
(33) Kamachi, M.; Yamada, B. *Polymer Handbook*, 4th ed.; Brandrup, J., Immergut, E. H., Grulke, E. A., Eds.; Wiley: New York, 1999.
(34) Tsarevsky, N.; Pintauer, T.; Matyjaszewski, K. *Macromolecules* **2004**, *37*, 9768−9778.
(35) Kickelbick, G.; Pintauer, T.; Matyjaszewski, K. *New J. Chem.* **2002**, *26*, 462−468.
(36) Bashir, W.; Tyrrell, E.; Feeney, O.; Paull, B. *J. Chromatogr., A* **2002**, *964*, 113−122.
(37) Gopireddy, D.; Husson, S. M. *Macromolecules* **2002**, *35*, 4218−4221.
(38) Matyjaszewski, K.; Nanda, A. K.; Tang, W. *Macromolecules* **2005**, *38*, 2015−2018.
(39) Kim, J.; Huang, W.; Miller, M.; Baker, G.; Bruening, M. *J. Polym. Sci.: Part A: Polym. Chem.* **2003**, *41*, 386−394.
(40) Dubois, L. H.; Nuzzo, R. G. *Annu. Rev. Phys. Chem.* **1992**, *43*, 437−463.
(41) Matyjaszewski, K. *Curr. Org. Chem.* **2002**, *6*, 67−82.
(42) Coullerez, G.; Carlmark, A.; Malmström, E.; Jonsson, M. *J. Phys. Chem. A* **2004**, *108*, 7129−7131.
(43) Samadi, A.; Husson, S. M.; Liu, Y.; Luzinov, I.; Kilbey, S. M., II. *Macromol. Rapid Commun.* **2005**, *26*, 1829−1834.

MA0519361